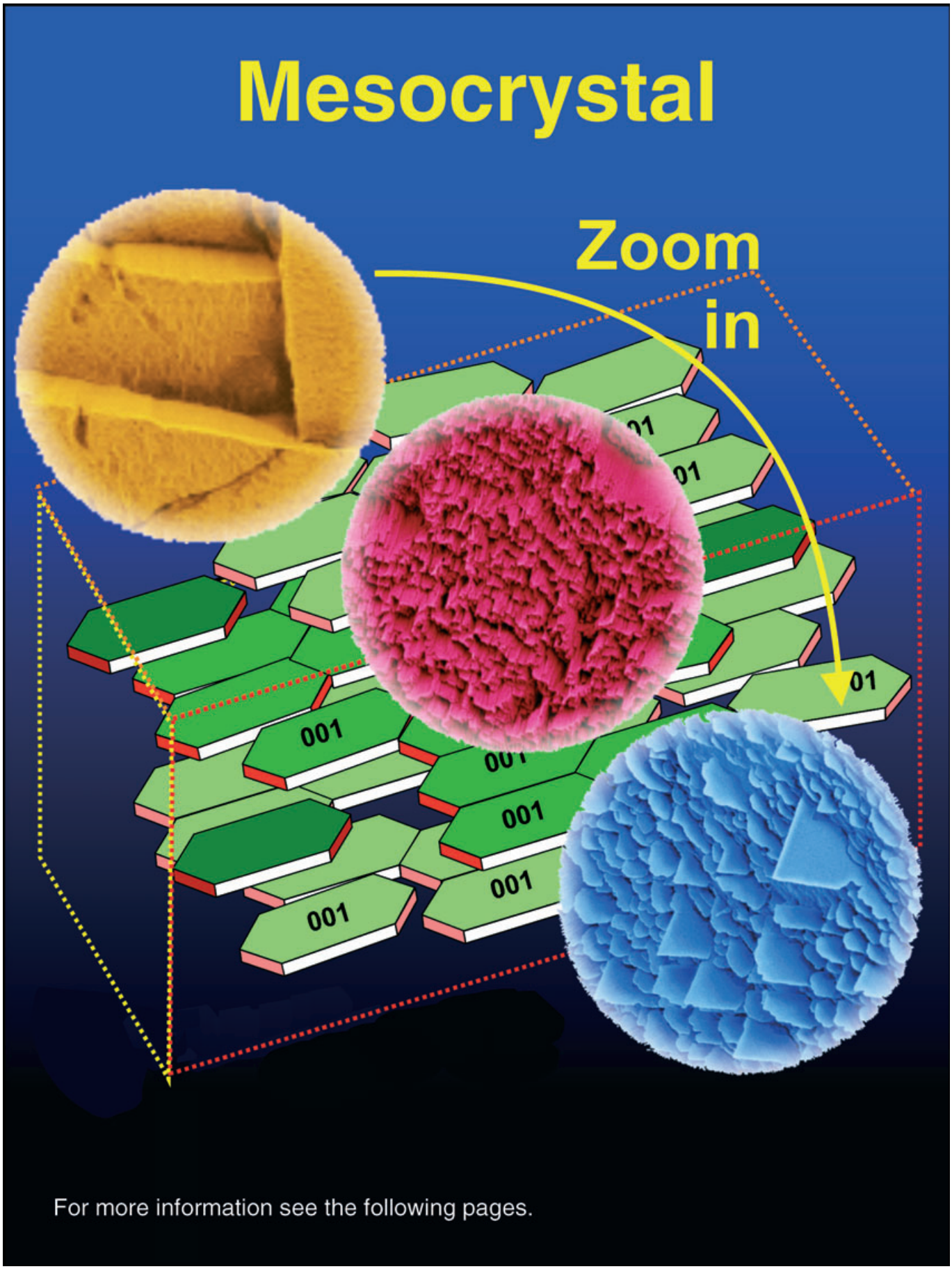

Chem. Eur. J. **2005**, *11*, 2903 – 2913 **DOI: 10.1002/chem.200400420**

CHEMISTRY
A EUROPEAN JOURNAL

Polymer-Induced Alignment of DL-Alanine Nanocrystals to Crystalline Mesostructures

Sebastian Wohlrab,[a] Nicola Pinna,[b] Markus Antonietti,[b] and Helmut Cölfen*[b]

Abstract: Crystallization of DL-alanine by cooling of a supersaturated solution in the presence of a chiral double-hydrophilic block copolymer poly(ethylene glycol)-*block*-poly(ethylene imine)-*S*-isobutyric acid (PEG_{4700}-PEI_{1200}-*S*-*i*BAc) yields crystal superstructures with an astonishing morphology. Although analysis by light microscopy reveals these crystals to be apparently well facetted, electron microscopy shows that they consist of three-dimensionally, well-aligned nanocrystals that are scaffolded to a so-called mesocrystal. This mesocrystal is formed by polymer-mediated structuration, and provides evidence for the importance of mesoscopic events in a typical crystallization process.

Keywords: alanine · copolymers · crystal engineering · crystal growth · mesocrystal

Introduction

The structuration of nanoparticles into ordered superstructures by using bottom-up approaches is one of the key topics of modern colloid and materials chemistry.[1] In this field, much can be learned from the processes of biomineralization that yield well-defined, organic–inorganic hybrid materials with superior materials properties, complex morphologies, and hierarchical order.[2–4]

One of the fundamental aspects of bio- and biomimetic mineralization is the possibility of a mesoscopic ordering of materials through self-organization and transformation.[5] Even conventional crystallization processes are considered to be more than just the formation of a solution-mediated lattice from ions. Aggregation-mediated crystallization via mesoscopic building units seems to be relevant in many cases;[5] for example, iron oxides,[6] cerium oxide,[7] copper oxalates,[8] and copper oxides[9] are all solids containing metal ions that readily undergo hydrolytic polymerization and cluster formation in aqueous solution. The current theory, with its two principal paths of crystallization, is represented in Figure 1, left and center.

[a] Dr. S. Wohlrab
Institute of Inorganic Chemistry, Technical University of Dresden
Mommsenstrasse 13, 01069 Dresden (Germany)

[b] Dr. N. Pinna, Prof. Dr. M. Antonietti, Dr. H. Cölfen
Max-Planck-Institute of Colloids and Interfaces
Colloid Chemistry, Research Campus Golm
14424 Potsdam (Germany)
Fax: (+49) 331-567-9502
E-mail: helmut.coelfen@mpikg-golm.mpg.de

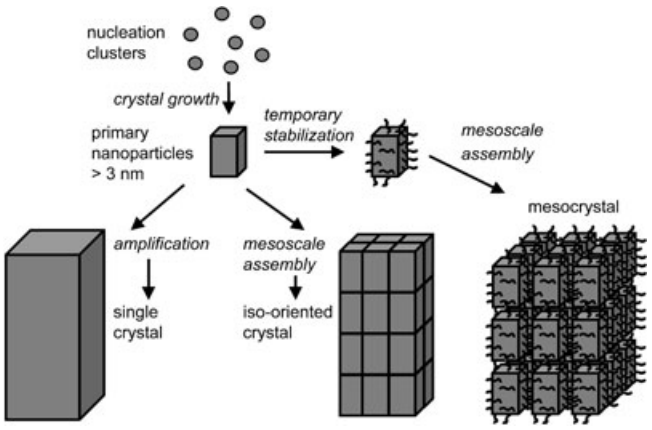

Figure 1. Alternative growth mechanisms of a crystal and a mesocrystal, partially adapted from reference [5].

The influence of polymers on crystal formation is usually attributed to their selective adsorption and/or enrichment onto specific crystal faces, similar to that seen with low molecular weight ionic compounds, which inhibits the growth of these faces.[10] Self-assembled and highly oriented superstructures can form through that approach, as was shown for a variety of ZnO superstructures obtained with a citrate additive.[11]

Polymers can also decrease colloidal stability, which induces aggregation.[12,13] On the other hand, polymer–surface interactions that increase colloidal stability, thereby influencing the size and shape of the primary clusters, are also known.[14] Particularly effective steric stabilizers for inorganic crystals in aqueous systems are the so-called double-hy-

DOI: 10.1002/chem.200400420

drophilic block copolymers (DHBCs), which consist of a hydrophilic sticking block for the crystal and a second hydrophilic block that promotes water dispersion.[15]

Apart from the anisotropy of the shape, specific steric, van der Waals, and hydrophilic–hydrophobic interactions can organize the primary particles into a mesoscopic superstructure. An impressive example of the surfactant-mediated one- and two-dimensional structuration of $BaCrO_4$ and $BaSO_4$ nanoparticles, respectively, was reported by Mann and co-workers.[16,17] Even more demanding is the controlled, three-dimensional structuration of nanoparticles to microparticles with defined external faces. The three-dimensional structuration of μm-sized particles to ordered crystalline and facetted superstructures on surfaces has already been described (for a recent review, see reference [18]). The structuration of monodispersed spherical nano- or microparticles to colloidal crystals has also been investigated extensively (for a recent review, see reference [19]). Fewer studies of the three-dimensional structuration of nonspherical nanocrystals to facetted crystals have been reported.

These crystals consisting of nanocrystal aggregates are called mesocrystals (Figure 1). Such synthetic hybrid materials exhibiting defined crystal faces, but constructed from three-dimensionally, well-aligned nanocrystals, have already been described for calcium carbonate systems,[20–22] copper oxalate,[8] $BaSO_4$,[23] CdS,[24] and $CoPt_3$.[25] However, the formation mechanism of such mesocrystals is unknown, as are the reasons for the perfect alignment of the mesoscopic building units in symmetries different from those of the primary crystals.

In this paper, we present the first example of an organic mesocrystal constructed from neutral molecules, illustrating that such structures are not formed exclusively by inorganic matter and its high cohesion energy. Crystals of organic molecules have the advantage that they have lower lattice energies than their inorganic ionic counterparts, and provide additional crystallization control parameters, such as chirality or dipole–dipole interactions. Thus, the crystallization of polar organic molecules, such as amino acids, is appropriate for studying the effects and relevant parameters for the formation of mesocrystals, and the nature of the forces aligning the primary nanoparticles.

Experimental Section

All chemicals were purchased from Aldrich with a purity >99% and were used without further purification, unless otherwise stated. Double-distilled water was used for the preparation of the crystallization solutions.

Polymer synthesis

*Bromopoly(ethylene glycol) (**2**)*: Monomethoxypoly(ethylene glycol) (**1**) (PEG_{4700}-OH, 150 g, $M_w = 5000\ g\,mol^{-1}$, $M_n = 4700\ g\,mol^{-1}$) was dissolved in toluene (600 mL) and refluxed for 2 h, using azeotropic distillation to remove traces of moisture from the solution. After cooling to 35 °C, freshly distilled anhydrous triethylamine (20 mL, 144.3 mmol), and freshly distilled thionyl bromide (25 g, 120.2 mmol) dissolved in dry toluene (50 mL), were added dropwise at 35 °C over the course of 1 h, under continuous stirring in a dry nitrogen atmosphere. The reaction was completed by refluxing for 2 h. The triethylammonium bromide was removed by passing the hot solution through a sintered glass funnel (type 2) with an approximately 2–3 cm thick layer of Hyflo Super Cell diatomeous earth. After cooling to 50 °C, active carbon was added (50 g). After filtration over a diatomeous earth layer and elution of the filtercake with hot toluene, the filtrate was stored at 4 °C overnight to crystallize the product. Residues of the product were formed by constriction and crystallization of the supernatant toluene. The solid products were dissolved in refluxing ethanol and further active carbon was added (50 g). The solution was filtered as above, constricted, and the product was recrystallized twice at 4 °C. This was then washed with diethyl ether and dried in a vacuum dessicator to yield a pale yellow product (101 g).

Poly(ethylene glycol)-block-*poly(ethylene imine) (**3**)*: A solution of poly(ethylene imine) (50 wt%, 6 mL, $M_n = 1200\ g\,mol^{-1}$) (PEI_{1200}) was heated in toluene (100 mL) under reflux, using azeotropic distillation to remove traces of moisture from the solution. The water-free solution was concentrated to 20 mL and bromopoly(ethylene glycol) (**2**) (11 g) in THF (100 mL), and triethylamine (1 mL, 9.9 mmol) were added. The mixture was then heated under reflux for 6 h. The resulting triethylammonium bromide was separated by filtration. The organic phase was evaporated and traces of toluene were removed by azeotropic distillation with water. The polymer was isolated by freeze-drying and then analyzed by quantitative ^1H NMR spectroscopy by using the ratio of PEI and PEG protons. The blocking efficiency was >90%. ^1H NMR (D_2O): $\delta = 2.30$–2.90 (H-PEI), 3.40–3.80 ppm (H-PEG).

Poly(ethylene glycol)-block-*poly(ethylene imine)*-S-*isobutyric acid (**5**)*: Poly(ethylene glycol)-*block*-poly(ethylene imine) (**3**) (7 g) was dissolved in THF (350 mL), and triethylamine (9 g, 88.9 mmol) and the methyl ester of *S*-bromoisobutyric acid (7.5 g, 41.2 mmol) were added. The mixture was heated under reflux for 6 h and the resulting triethylammonium bromide was separated by filtration. The organic phase was evaporated and the solid product was dried in a vacuum dessicator. The solid was then dissolved in a water/methanol mixture (1:3, 160 mL), $LiOH{\cdot}H_2O$ (3.5 g, 83.3 mmol) was added, and the mixture was stirred for 2 h. The solution was then neutralized by adding 0.5 N HCl. After dialysing from low molecular weight components ($MWCO = 1000\ g\,mol^{-1}$), the solution was freeze-dried and characterized. ^1H NMR (D_2O): $\delta = 1.20$–1.35 (CH_3- from *S*-bromoisobutyric acid), 2.30–2.90 (H-PEI; CH_2-, CH- from *S*-bromoisobutyric acid), 3.40–3.80 ppm (H-PEG); PEI functionalization degree: 41% (from ^1H NMR spectroscopy and gravimetry of the byproduct triethylammonium bromide); ORD: $[\alpha]_D^{20} = 3.7$ mdeg (1 wt% solution at 1 cm), which qualitatively confirms the chirality of the prepared polymer.

Crystallization: An amount of polymer PEG_{4700}-PEI_{1200} or PEG_{4700}-PEI_{1200}-*S*-*i*BAc (10 or 100 mg, respectively) was added to a filtered, saturated, aqueous solution of DL-alanine (10 mL) at 65 °C, and allowed to dissolve as the mixture was cooled to room temperature. The solution was filtered and poured into a small bottle. After 24 h crystallization had started and was complete within 7 days. The crystals were then filtered from the solution, washed three times with ethanol, and dried at 50 °C under vacuum, before being analyzed by using light microscopy.

Analytical methods: The NMR spectroscopy experiments were performed by using a Bruker DPX-400 instrument at 25 °C with D_2O as solvent. Both light microscopy of solutions and scanning electron microscopy (SEM) were applied to all samples. The use of light microscopy is necessary to prove that the SEM micrographs show real structures instead of drying artefacts that result from sample preparation. The SEM measurements were performed by using a LEO 1550-GEMINI microscope. Light microscopy images were recorded in solution by using an Olympus BX50 instrument. Powder X-ray diffraction (XRD) patterns were recorded by using a PDS 120 diffractometer (Nonius, Solingen) equipped with $Cu_{K\alpha}$ radiation. The ω scan-mode crystal analysis with crystal rotation along [001] was performed by using a Bruker-AXS, Modell SMART. The surface cleavage of the crystal faces, the cell structure, and the modeling of morphologies were performed by using *C*erius^2 software (Accelrys). For the equilibrium growth morphology calculation in vacuum, the auto force field was enabled. The morphologies were then adapted to those ob-

served experimentally, by altering the distances between the faces and the virtual crystal center.

Results and Discussion

Polymer synthesis: As a suitable polymer for the crystallization of DL-alanine, a standard double-hydrophilic block copolymer (DHBC) was prepared and functionalized by using principles reported previously.[15,26,27] Poly(ethylene glycol)-*block*-poly(ethylene imine) (**3**) was employed as a backbone, and was synthesized by coupling the two polymer segments, which had molar masses of $M_n = 4700$ and 1200 g mol^{-1}, respectively (PEG_{4700}-PEI_{1200}). Monomethoxypoly(ethylene glycol) (PEG_{4700}-OH) (**1**) was activated by reaction with thionyl bromide under reflux conditions, using an excess of triethylamine in toluene to give the brominated telechelic species (PEG_{4700}-Br) (**2**), which has a functionalization degree of 100%.[28] This compound was coupled to a branched PEI with a molar mass of $M_n = 1200$ g mol^{-1} (PEI_{1200}), as this was shown by earlier investigations to provide a higher functional group density on a crystal surface than the linear or dendritic analogues.[29]

The AB-block structure (**3**) was obtained by refluxing an excess of 100% PEI_{1200} with PEG_{4700}-Br (**2**) in THF. The surplus of PEI was quantitatively removed by performing exhaustive dialysis (MWCO = 3000 g mol^{-1}). Gel permeation chromatography (GPC) revealed a blocking efficiency of 90% and a PEG contamination of about 10%, resulting from the nonquantitative yield of both reaction steps. The PEG homopolymer, however, is inert and does not disturb the subsequent crystallization examination, as earlier investigations have shown.[30]

To activate this polymer backbone, it was functionalized with appropriate sticker groups that can interact efficiently and selectively with appropriate crystal surfaces. This is only possible to a certain degree, as PEI consists of 25% primary, 50% secondary, and 25% tertiary amines.[31] The alkylation of the PEG_{4700}-PEI_{1200} in THF with the methyl ester of *S*-bromoisobutyric acid yielded a functionalized DHBC (**4**) with a functionalization degree of 41%, as revealed by ^{1}H NMR spectroscopy and gravimetric investigations of the byproduct triethylamine bromide, and implies that all primary and some secondary amine groups were functionalized. This conversion is typical for polymer reactions with PEI.[27] Subsequent cleavage of the ester produced a zwitterionic chiral DHBC (**5**), which is suitable for the crystallization of amino acids, in this case DL-alanine (Scheme 1).

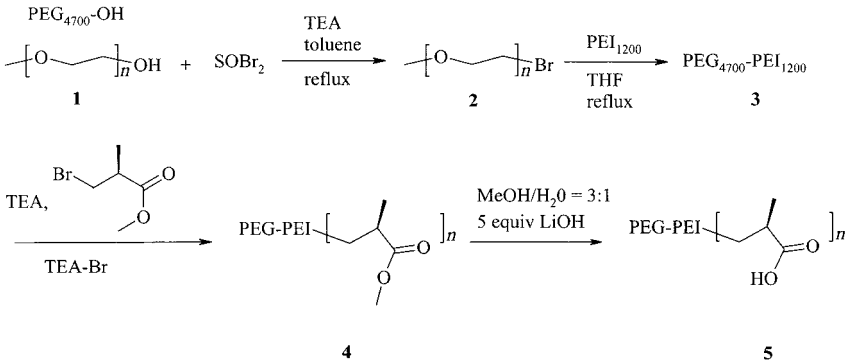

Scheme 1. Reaction scheme for the preparation of PEG_{4700}-PEI_{1200}-*S*-*i*BAc.

Crystallization: DL-alanine crystallizes from aqueous solution in the space group $Pna2_1$ with an orthorhombic unit cell.[32] Free crystallization of a supersaturated DL-alanine solution in bidistilled water by cooling from 65 to 20 °C yields needlelike racemic crystals within a few hours (Figure 2a). In the presence of 0.1 wt% PEG_{4700}-PEI_{1200}, which is the nonfunctionalized DHBC backbone, a nonspecific change in the crystals is observed. Instead of the original filigree needle, a compact rectangular structure with sharp side-faces and irregular tips is obtained (Figure 2b). The thickness of the crystals is increased by a factor of ten compared to the default experiment, and a vague central inner structure is apparent. The addition of functionalized DHBC PEG_{4700}-PEI_{1200}-*S*-*i*BAc at a concentration of 0.1 wt% shows a much stronger influence on crystallization. The original needle form disappears completely in favor of bricklike crystal bodies with irregular morphology (Figure 2c).

The strong morphology-directing effect of the block copolymer with its chiral sticker groups is clear, and nicely supports the DHBC concept, as previously applied to inorganic compounds, such as $CaCO_3$,[27,33–38] $Ca_x(PO_4)_y(OH)_z$,[30] $BaSO_4$,[39–44] $BaCrO_4$,[45,46] ZnO,[47–50] CaC_2O_4*$2H_2O$,[51] CdWO4,[52] and lanthanides[53] or Au.[54] Chiral aspects during the crystallization have been examined mainly by the Lahav group.[55–57]

To examine the role of chirality, we investigated the influence of this polymer on the crystallization kinetics of the enantiopure amino acids. The presence of 0.1 wt% of PEG_{4700}-PEI_{1200}-*S*-*i*BAc results in a significant change in the crystallization kinetics, as revealed by measurements of the circular dichroism ($\lambda = 240$ nm) of the supernatant solution over time (Figure 3). Although the growth of L-alanine is slowed down by the polymer, the D-alanine growth rate is accelerated. This dependence proves the "rule of reversal",[55,58] that is, the polymer binds better to a surface of equal chiral character, so that this surface becomes inhibited and the other enantiomer preferentially crystallizes. The temporary separation of enantiomers was recently observed for tartrate salts with a chiral DHBC,[58] in which the racemate and the enantiopure compounds were nevertheless thermodynamically very similar and had a similar free enthalpy of crystallization. However, performing similar circular dichroism measurements on the supernatant solution of

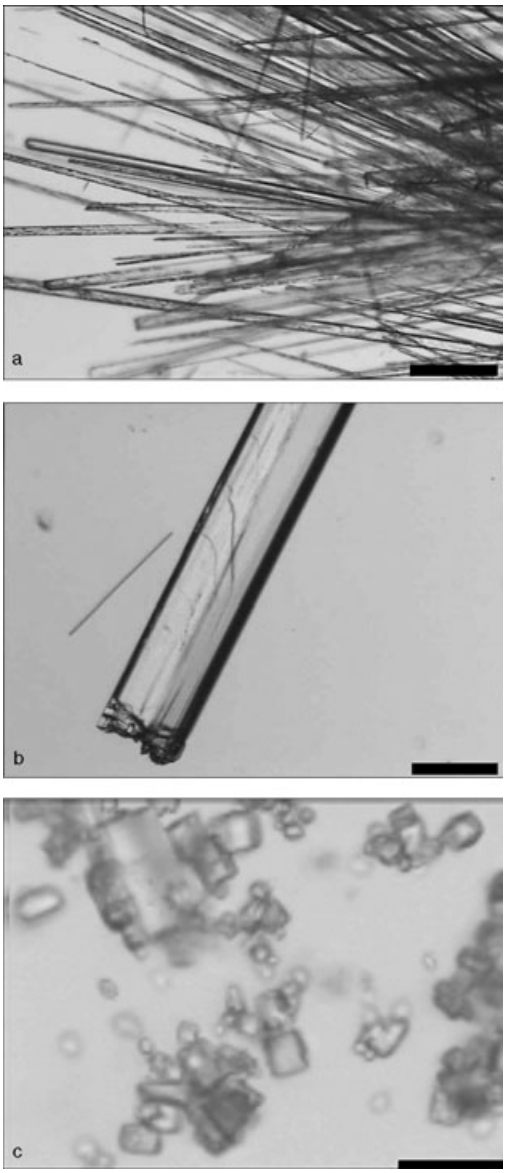

Figure 2. Light micrographs showing DL-alanine crystals obtained by cooling a supersaturated solution from 65 to 20 °C; a) default experiment without additive (scale bar = 200 μm), b) a crystal obtained by addition of 0.1 wt % PEG_{4700}-PEI_{1200} (scale bar = 200 μm), and c) crystals obtained by addition of 0.1 wt % PEG_{4700}-PEI_{1200}-*S*-*i*BAc (scale bar = 20 μm).

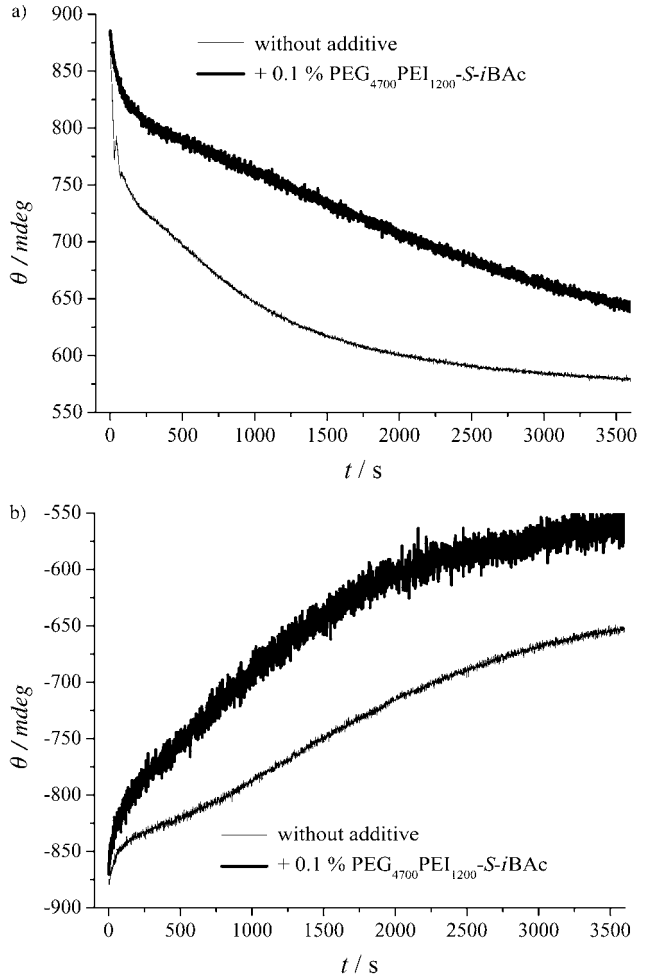

Figure 3. Kinetic measurements of the crystallization of the alanine enantiomers by using circular dichroism detection of the supernatant; a) L-alanine, b) D-alanine. Crystallization was induced by the abrupt cooling of a supersaturated solution from 85 to 20 °C. The diagrams compare the free crystallization with that in the presence of 0.1 wt % PEG_{4700}-PEI_{1200}-*S*-*i*BAc.

a 1:1 mixture of D- and L-alanine, with 0.1 wt % polymer as in Figure 3, reveals no change in the optical rotation over time (it is still the racemate that is crystallizing), and no chiral separation was achieved. Clearly, the polymer can differentiate between the two enantiomers; nevertheless, it binds with similar strength to faces of the racemate crystals, so that this thermodynamically more stable species prevails. We can conclude, therefore, that the novel structures are also composed of racemic crystals.

A higher resolution picture of the crystals obtained in the presence of the PEG_{4700}-PEI_{1200}-*S*-*i*BAc additive shows the detailed nature of the products (Figure 4a). Although the "crystals" are apparently well facetted, they show an inner texture and cracks, and are clearly composed of many small tectons. Sites parallel to the longitudinal axis display smooth surfaces, whereas sites on the lateral axis have a rough shape and show structuring. The wavy surfaces and irregular edges observed are atypical for single crystals and are likely to be the effect of an imperfect structuring of subunits. In addition, tension cracks can be observed.

To obtain more information about the inner texture of these superstructures, an etching experiment was performed by refluxing the crystals for 8 h in the nonsolvent methanol. The block copolymer within the crystal partly dissolved, and the resulting, less-fixed structures reveal their inner connectivity. Figure 4b shows the coupled SEM results revealing a porous structure. The initially smooth surface became textured and less regular. A reference experiment for a DL-alanine single crystal boiled in methanol under the same conditions still yielded a crystal with smooth surfaces (Figure 4c), which clearly reveals that the cavities in Figure 4b must

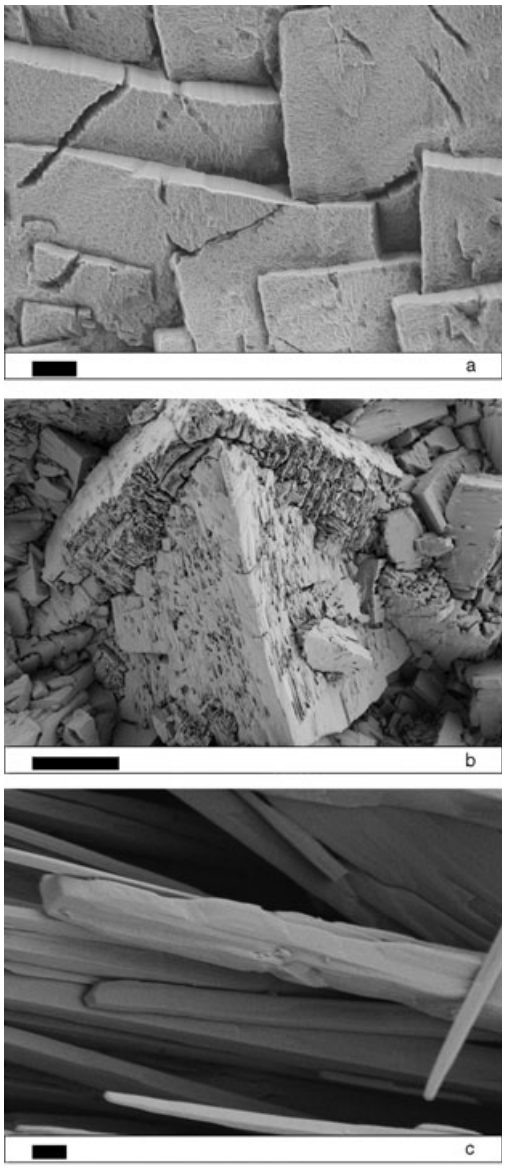

Figure 4. SEM images of DL-alanine crystals; a) obtained by addition of 0.1 wt% PEG_{4700}-PEI_{1200}-*S*-*i*BAc at high resolution (scale bar = 2 μm), b) after etching for 8 h in refluxing methanol (scale bar = 200 μm), and c) default experiment with single crystals (scale bar = 1 μm).

result from polymer dissolution, despite the possible slight dissolution of alanine.

Upon increasing the concentration of polymer PEG_{4700}-PEI_{1200}-*S*-*i*BAc to 1 wt%, a more regular, cubic crystal morphology is obtained (Figure 5a), in which all edges have a similar length of between 50 and 100 μm. The reason for the more uniform shape may be a higher order of the nanocrystals in the compound structure and will be discussed in more detail below. One set of the orthogonal faces shows smooth surfaces, one set is slightly striated, and one set of the cubic faces is rough and exhibits pronounced surface structure. In addition to the cubes, fused, cross-grown mesocrystals are found. In contrast to the crystals obtained with the lower concentration of polymer (Figure 4), no cracks are observed

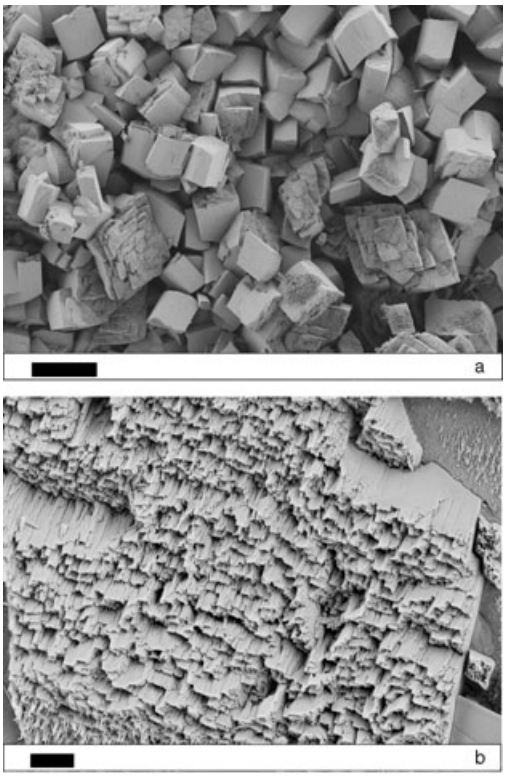

Figure 5. a) SEM image of DL-alanine crystals formed by crystallization of 10 mL of a supersaturated solution (cooled from 65 to 20 °C by addition of 1 wt% PEG_{4700}-PEI_{1200}-*S*-*i*BAc) (scale bar = 100 μm). b) The view of one of the rougher faces revealing the inner mesostructure (scale bar = 2 μm).

in the mesocrystals, indicating a more pronounced inner texturation.

Higher resolution SEM pictures of the rough sites of less-perfect species reveal the inner alignment of the nanocrystals within these superstructures (Figure 5b). Very thin, platelet-like crystals, aligned along their *c* axis to a multilayer stack (for mesocrystal face-indexing, see Figures 10 and 11), constitute the complete mesocrystal and are aligned perpendicular to the rough face. From these pictures, the thickness of the primary crystals can be estimated to be below 100 nm. Although a dense packing of needles would also be compatible with the observations in Figure 5b, the following results strongly suggest that the primary particles are platelets that can form needles by oriented attachment. The primary crystals are well separated, indicating the presence of tightly bound, intracrystalline polymers; that is, the whole structure is a layered nanocomposite.

We also tried to embed the crystal superstructures into epoxy to obtain microtome sections. Due to the low stability and high brittleness of the compound structure, precise cutting in all directions is not possible, and mostly fragments of destroyed mesocrystals are observed. The three-dimensionally aligned lamellar structure of the mesocrystals is demonstrated in Figure 6. Although the exact orientation of this thin cut is unclear, the high level of subunit orientation within a mesocrystal is apparent. The mesocrystal has essen-

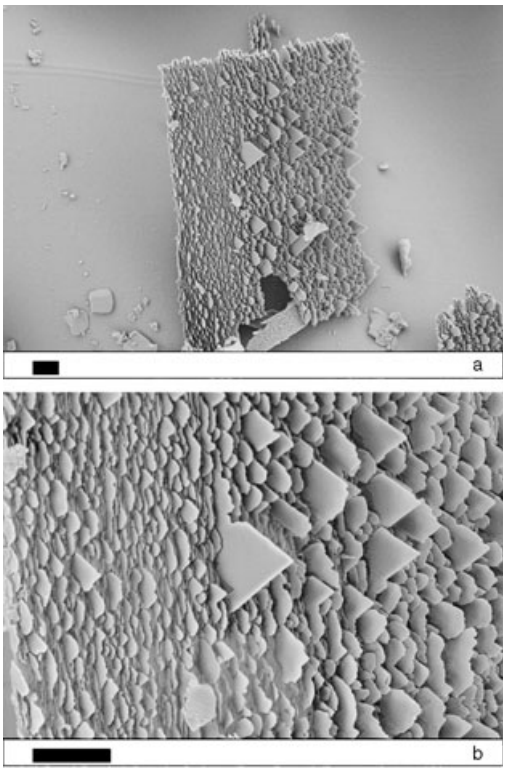

Figure 6. a) SEM image of DL-alanine crystals formed by crystallization of 10 mL of a supersaturated solution (cooled from 65 to 20 °C by the addition of 1 wt % PEG_{4700}-PEI_{1200}-*S*-*i*BAc) showing the semicut mesostructure (scale bars = 3 μm). b) Close up of part of image in (a).

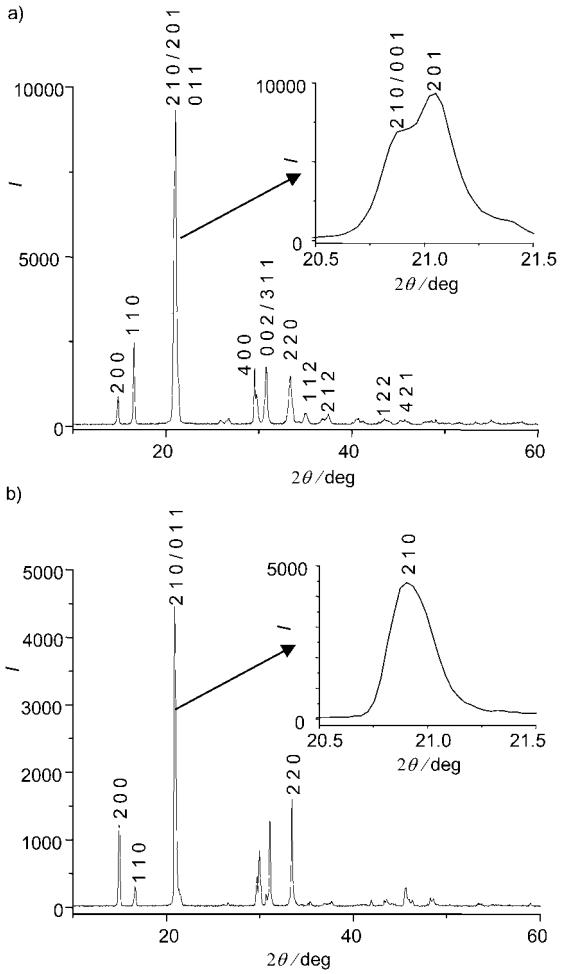

Figure 7. Results of WAXS analysis of DL-alanine crystals formed by the crystallization of 10 mL of a supersaturated solution (cooled from 65 to 20 °C); a) default experiment in the absence of additive, b) following the addition of 1 wt % PEG_{4700}-PEI_{1200}-*S*-*i*BAc.

tially a rectangular cross-section, in which the single crystalline lamellae are parallel to the flat outer surfaces of the mesocrystal. Remarkably, all of the single nanocrystal plate units have the same fracture texture and angles, emphasizing that each nanocrystal is vectorially well aligned with respect to the next crystal; that is, the mesocrystal possesses a common coordinate system. This texture provides relevant information concerning the action of the polymer and the architectural principles of the mesocrystal.

Despite the large morphological differences between the single reference crystal of DL-alanine and the mesocrystal, there are only minor differences in the wide-angle X-ray scattering (WAXS) results (Figure 7). Even the porous structures formed at low concentrations of polymer show well-developed scattering peaks that are very narrow. Amorphous domains within the structures are clearly absent. Both crystals can be indexed according to the orthorhombic primitive lattice, which is known for DL-alanine. The difference between the two diffractograms is subtle, despite the observation of orientational effects in the powder diffractogram upon repetition of the experiment. The absence of peaks or a decrease in peak intensities indicates the substructure of the mesocrystal, or the structure of the primary nanoparticles, respectively. The (200) peak is increased, whereas the (110) peak is decreased. Although the sample was measured as a powder, orientational effects cannot be completely excluded. Higher resolution of the area around 21° (Figure 7b, inset) illustrates the absence of the original (201 and 011) scattering peak. The standard explanation for the absence of peaks, but the preservation of crystal structure, is an altered exposure of faces. The disappearance of the main scattering peak and the shifts in intensity occur because certain crystal directions exist in only nanometer dimensions. This is evident from the observed "vanishing of peaks" due to very broad peak widths, and leads to the peak disappearance in the baseline.

On the basis of these results, it is possible to develop a molecular mechanistic understanding of the interaction and structuration process. It is already known that DL-alanine is a polar crystal along the *c* axis; it displays well-developed "capped (201) and (011) faces" at one end of the polar *c* axis where $-NH_3^+$ groups are exposed, and at the opposite flat (00-1) face, $-COO^-$ groups are exposed.[59–61] We have depicted the molecular surface structure of DL-alanine, as viewed along the *b* and *c* axis, by using the program *C*erius[2] (Figure 8). The effects of surface reconstitution and hydra-

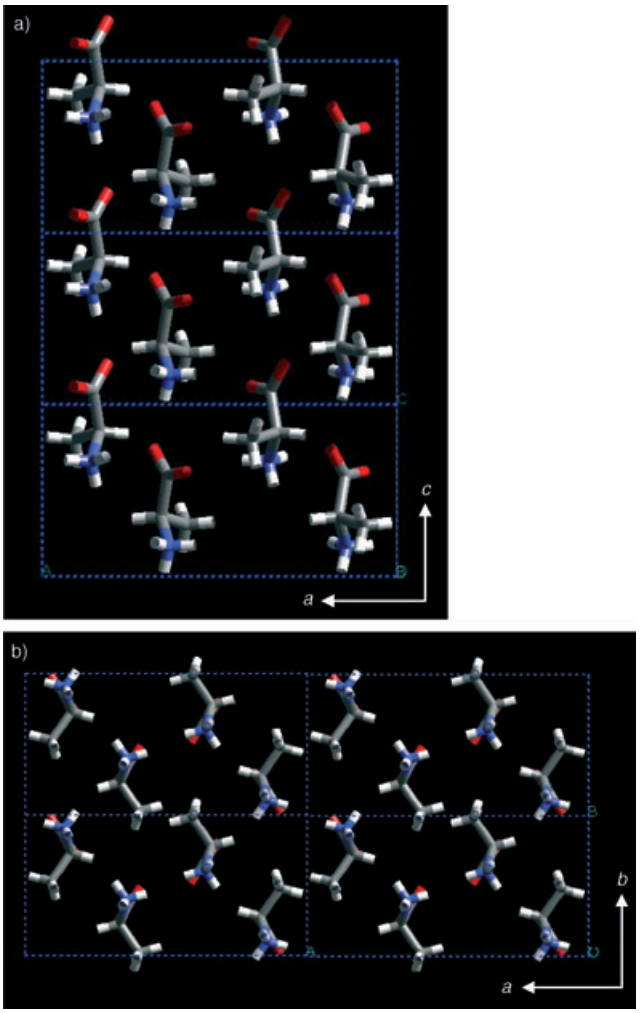

Figure 8. Molecular surface structure of DL-alanine viewed along the *b* axis (a) and *c* axis (b). Gray = carbon, red = oxygen, blue = nitrogen.

tion were not considered; the surfaces were constructed simply from the well-known unit cell of DL-alanine.

The (200) and (210) faces are similar; both show cationic, anionic, and nonpolar methyl groups as surface sites in equal proportions. Interestingly, despite the decrease in the (110) peak, the relative intensity of the related (220) peak increases (Figure 7). The reason for this is unknown, but suggests orientational effects. A similar situation exists for the (210) surface, which is a morphology-determining face due to its slow growth. That this is an exposed face could explain why this peak is so strong in both the reference sample and the mesocrystal. The (201) and (011) faces can be easily identified as polar surfaces, from which four amino units per unit cell extrude.[59–61] The most polar surface, however, is the (001) face. Because the *c* axis in DL-alanine is the dipole axis, the (001) face is polar, with one side rich in carboxylic acids and the counterface rich in amines.

The acidic polymer can interact with the faces that exhibit amino groups; predominately (001). The relative occupation depends on polymer concentration, but the experiments show that at the low polymer concentrations used, the (001) face is preferred, which makes this usually unexposed face dominant in the initially formed nanocrystals.

The DL-alanine morphologies observed for the single crystal, based on the work of Lahav and co-workers[59–61] (Figure 9a), and the suggested morphology of the primary building unit of the mesocrystals (Figure 9b), demonstrate the morphology changes to the latter. Instead of the needlelike structure obtained in the absence of polymer (Figure 9a), the lowering of interface energies by polymer adsorption, as discussed, results in a platelet with strongly exposed (001) and (00-1) faces. Around the rim of the platelet, there are two 90° and four 135° angles. Due to the lowering of the (001) interface energies by polymer adsorption, the initially slow-growing (210) and (200) faces become relatively fast growing with respect to (001).

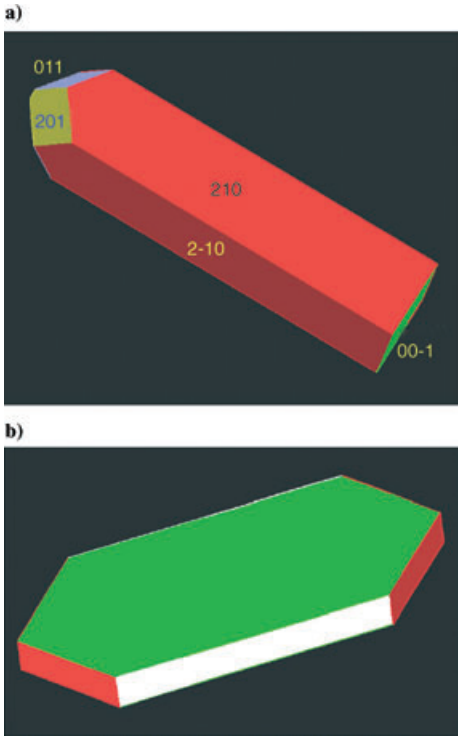

Figure 9. DL-alanine crystals formed by the crystallization of 10 mL of a supersaturated solution (cooled from 65 to 20 °C) (red = (210), white = (200), blue = (011), yellow = (201), green = (001); a) default experiment in the absence of additive based on the work of Lahav and co-workers,[59–61] b) suggested mesocrystal subunit obtained by the addition of 1 wt % PEG_{4700}-PEI_{1200}-*S*-*i*BAc. The morphology of the mesocrystal subunits in (b) was drawn on the basis of experimentally observed faces.

On the basis of this elementary unit, the architecture of the mesoscale superstructure is simple to explain: The whole structure is oriented in the [100], [010], and [001] directions, with the *z* direction being the stacking plane. In the *x* direction, the primary crystals also have a flat side, albeit with stacking irregularities (striations). The mesocrystal, however, must be rough in the *y* direction, as the (010) face is not exposed in the building units.

The polar character of the (001) and (00-1) faces (one side amine, one side carboxyl groups) is very important for the construction of the superstructure: the simple plates are held together by strong dipole–dipole interactions, which cummulate from unit cell to unit cell over the whole plate thickness so that the whole superstructure is polar. As the mesocrystals do not cleave along those lines, as might be expected, the cohesive force perpendicular to the plates must be quite high. Furthermore, the fairly constant thickness of the plates in nanodimensions may be explained by the dipolar character; such supramolecular dipole moments are usually growth-limited to a critical value and a corresponding mesoscopic structural length, otherwise the coupled forces become too high.

To support the high vectorial alignment of the primary nanocrystalline units observed and the indexing of the outer faces, one selected mesocrystal was subjected to an XRD ω-scan crystal analysis, in which the crystal was rotated around its [001] axis (Figure 10, for a simple comparison, only one iso-oriented scattering plane is presented). The diffraction images of the mesocrystal (Figure 10a) are indeed comparable to the diffraction of a DL-alanine single crystal (Figure 10b). The diffraction spots are defined and only slightly smeared, indicating some type of structural flexibility within the compound structure, with minor fluctuations in orientation around a common axis. It was already seen in the SEM pictures that the outer faces are not exactly parallel, but can exhibit a slightly curved appearance and angular fluctuations. The mesocrystals clearly contain larger amounts of polymer and are composite structures with intermediate softness. The smearing of the peaks is only minor, and depends on orientation (in accordance with a tensorial plasticity), but is below 5°.

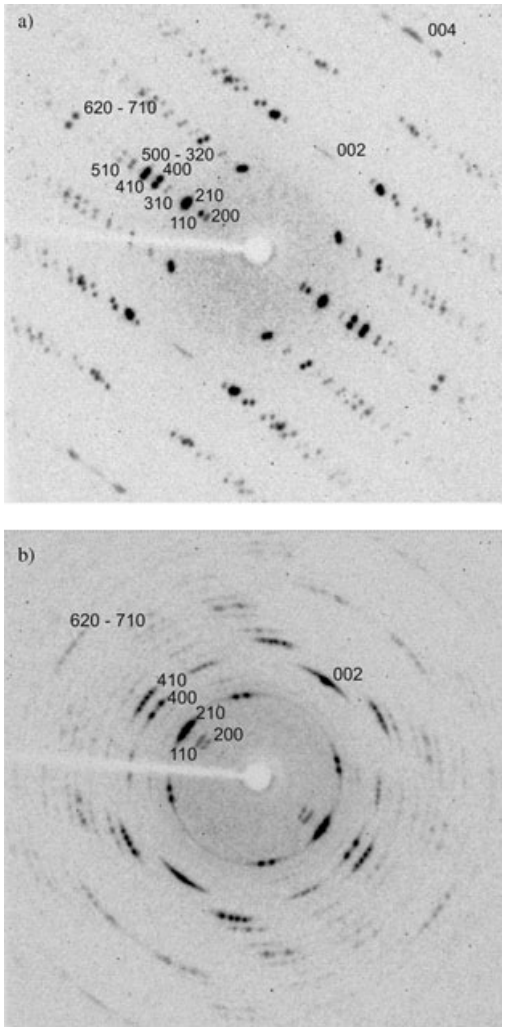

Figure 10. X-Ray analysis of DL-alanine (ω-scan rotated along [001]); a) DL-alanine mesocrystal, b) DL-alanine single crystal.

The "single crystal" is found to be twinned, most presumably along the [00-1] dissymmetry (see Figures 9 and 10) to compensate dipole moments, as the twinning is maximal perpendicular to the [001] direction. In addition, the XRD image of the mesocrystal contains some specific features. The stacking of the plates along the [001] axis in the mesocrystal highly intensifies the (002) reflection, but weakens the (004) reflection. This is typical for lattice defects in this direction, presumably due to the incorporation of polymer into the crystalline structure. The twinning now takes place in quads, which is interpreted as all four principal orientations of the primary nanoplatelets occurring with similar probability in the mesocrystals.

Conclusion

The crystallization of DL-alanine in the presence of the double-hydrophilic block copolymer poly(ethylene glycol)-*block*-poly(ethylene imine)-*S*-isobutyric acid yielded well-facetted superstructures. These were shown to be mesocrystals; that is, regular scaffolds composed of well-separated, but almost perfectly three-dimensionally aligned, nanocrystals with a platelet-like shape. We propose a hexagonal (001) platelike morphology for the nanocrystals with four (210) and two (200) side faces, in which the former (210) was also observed in the reference crystal and the latter (200) is energetically stable. We could not assign the Miller indices to the nanocrystals.

Although a clear layered nanostructure with intercalated polymer was observed in the polar *c* direction, in the *a* and *b* directions the crystals appear to fuse together to form larger, single crystalline platelets, probably by an oriented attachment mechanism[62] of the neutral (210) and (200) faces.

The main stimulus for the cascade of crystalline mesostructure formation is polymer adsorption onto the highly polar, otherwise unexposed (001) face of the DL-alanine crystals, as illustrated by computer modeling using *C*erius[2]. The resulting platelet-like crystals probably show a strong dipole moment normal to the platelet direction, which drives the stacking process in the [001] direction. It was also demonstrated by using surface plane cuts that the polymer employed does not significantly adsorb onto the (210) and

(200) faces, making them high in surface energy relative to the (001) face. This probably induces crystallographic fusion by means of oriented attachment in the layers. Throughout this process, redistribution of matter results in inclusions and defects, which also limits the entire fusion within the single layers. The entire self structuration mechanism is schematically shown in Figure 11.

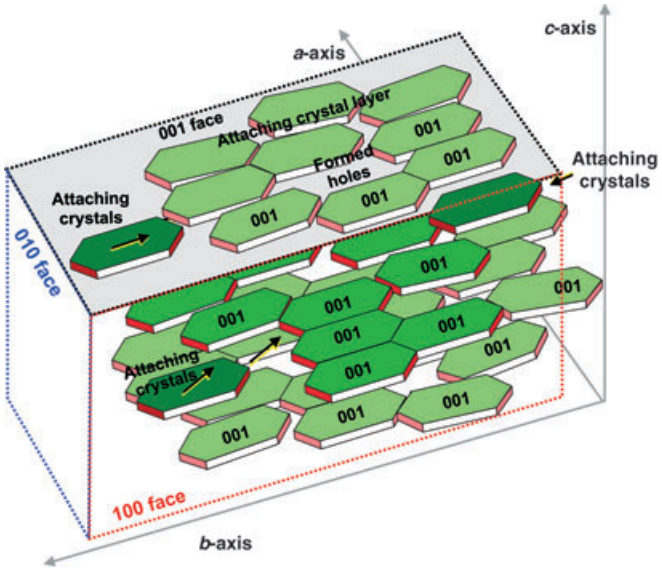

Figure 11. Schematic drawing of the self-structuration of a primary crystal to a mesocrystal for DL-alanine, with an outline of the externally exposed faces. Note that the rough face is (010), which exposes the nanocrystal platelet tips. Along the *a* and *b* directions partial particle fusion occurs by oriented attachment. For simplicity, the polymer is not shown.

Interestingly, results of both SEM and XRD analysis indicate a certain structural flexibility. Many mesocrystals were found to have bent and curved surfaces, and XRD studies showed that, apart from minor angular smearing, many peaks occur in well-defined quadruplets. This was interpreted as multiple twinning between the single nanoplatelet tectons, which can occur in four principal directions.

Finally, due to the compensation of many growth effects, the mesocrystals adopt a cubelike shape exposing the three basal planes (Figure 11). Remarkably, this simple cubic superstructure observed experimentally is not encoded in the primary primitive orthorhombic unit cell symmetry of the crystal (space group $Pna2_1$); that is, it presumably results from the averaging out of different orientations, to give an overall supersymmetry that is simple.

The mesocrystals are clearly soft hybrid structures, a new principle of organization between liquid crystals and crystals, and are formed by a polymer-mediated structuration process. Because the underlying principles of the interaction of primary nanocrystals into larger units are not restricted to polymer-bound species, this also suggests the importance of mesoscopic processes in more simple crystallization events.

The importance of electric fields and electric binding on structure formation will be addressed in future work by performing similar studies in outer electric fields and in the presence of salts.

As the resulting superstructures are both "soft" and polar aligned in [001] direction, this system is also a promising candidate for organic piezoelectricity.

Acknowledgements

We thank the Max-Planck Society for financial support. We also thank A. Thünemann and G. Reck for close cooperation with the ω-scan crystal diffraction experiments and for helpful discussions. M. Page is acknowledged for careful proofreading of this manuscript.

[1] M. Antonietti, G. A. Ozin, *Chem. Eur. J.* **2004**, *10*, 28–41.
[2] H. A. Lowenstam, S. Weiner, *On Biomineralization*, Oxford University Press, New York, **1989**.
[3] S. Mann, *Biomineralization*, Oxford University Press, Oxford, **2001**.
[4] E. Bäuerlein, *Biomineralization*, Wiley-VCH, Weinheim, **2000**.
[5] H. Cölfen, S. Mann, *Angew. Chem.* **2003**, *115*, 2452–2468; *Angew. Chem. Int. Ed.* **2003**, *42*, 2350–2365.
[6] E. Matijevic, P. Scheiner, *J. Colloid Interface Sci.* **1978**, *63*, 509–524.
[7] W. P. Hsu, L. Ronnquist, E. Matijevic, *Langmuir* **1988**, *4*, 31–37.
[8] N. Jongen, P. Bowen, J. Lemaître, J. C. Valmalette, H. Hofmann, *J. Colloid Interface Sci.* **2000**, *226*, 189–198.
[9] S. H. Lee, Y. S. Her, E. Matijevic, *J. Colloid Interface Sci.* **1997**, *186*, 193–202.
[10] J. H. Adair, E. Suvaci, *Curr. Opin. Colloid Interface Sci.* **2000**, *5*, 160–167.
[11] Z. R. R. Tian, J. A. Voigt, J. Liu, B. McKenzie, M. J. McDermott, M. A. Rodriguez, H. Konishi, H. F. Xu, *Nat. Mater.* **2003**, *2*, 821–826.
[12] B. Vincent, "The Stability of Solid/Liquid Dispersions in the Presence of Polymers", in *Solid/Liquid Dispersions* (Ed.: T. F. Tadros), Academic Press, London, **1987**.
[13] G. J. Fleer, M. H. Cohen Stuart, J. M. H. Scheutjens, T. Cosgrove, B. Vincent, *Polymers at Interfaces*, Chapmann Hall, **1993**.
[14] D. H. Napper, *Polymeric Stabilization of Colloidal Dispersions*, Academic Press, London, **1983**.
[15] H. Cölfen, *Macromol. Rapid Commun.* **2001**, *22*, 219–252.
[16] M. Li, H. Schnablegger, S. Mann, *Nature* **1999**, *402*, 393–395.
[17] M. Li, S. Mann, *Langmuir* **2000**, *16*, 7088–7094.
[18] Z. R. Tian, J. Liu, J. A. Voigt, B. Mckenzie, H. Xu; *Angew. Chem.* **2003**, *115*, 430–433; *Angew. Chem. Int. Ed.* **2003**, *42*, 413–417.
[19] R. Anselmann, H. Winkler, *Adv. Eng. Mater.* **2003**, *5*, 560–562.
[20] J. Zhan, H. P. Lin, C. Y. Mou, *Adv. Mater.* **2003**, *15*, 621–623.
[21] O. Grassmann, R. B. Neder, A. Putnis, P. Löbmann, *Am. Mineral.* **2003**, *88*, 647–652.
[22] O. Grassmann, P. Löbmann, *Chem. Eur. J.* **2003**, *9*, 1310–1316.
[23] B. Judat, M. Kind, *J. Colloid Interface Sci.* **2004**, *269*, 341–353.
[24] T. Vossmeyer, G. Reck, L. Katsikas, E. T. K. Haupt, B. Schulz, H. Weller, *Science* **1995**, *267*, 1476–1479.
[25] E. V. Shevchenko, D. V. Talapin, A. L. Rogach, A. Kornowski, M. Haase, H. Weller, *J. Am. Chem. Soc.* **2002**, *124*, 11480–11485.
[26] M. Sedlak, M. Antonietti, H. Cölfen, *Macromol. Chem. Phys.* **1998**, *199*, 247–254.
[27] M. Sedlak, H. Cölfen, *Macromol. Chem. Phys.* **2001**, *202*, 587–597.
[28] A. F. Bückmann, M. Morr, G. Johansson, *Makromol. Chem.* **1981**, *182*, 1379–1384.
[29] L. M. Qi, H. Cölfen, M. Antonietti, *Nano Lett.* **2001**, *1*, 61–65.

[30] M. Antonietti, M. Breulmann, C. G. Göltner, H. Cölfen, K. K. W. Wong, D. Walsh, S. Mann, *Chem. Eur. J.* **1998**, *4*, 2493–2500.
[31] J. Suh, H. S. Park, *J. Polym. Sci. Part A: Polym. Chem.* **1997**, *35*, 1197–1210.
[32] J. Donohue, *J. Am. Chem. Soc.* **1950**, *72*, 949–953.
[33] H. Cölfen, M. Antonietti, *Langmuir* **1998**, *14*, 582–589.
[34] J. M. Marentette, J. Norwig, E. Stockelmann, W. H. Meyer, G. Wegner, *Adv. Mater.* **1997**, *9*, 647–651.
[35] H. Cölfen, L. M. Qi, *Chem. Eur. J.* **2001**, *7*, 106–116.
[36] J. Rudloff, M. Antonietti, H. Cölfen, J. Pretula, K. Kaluzynski, S. Penczek, *Macromol. Chem. Phys.* **2002**, *203*, 627–635.
[37] S. H. Yu, H. Cölfen, J. Hartmann, M. Antonietti, *Adv. Funct. Mater.* **2002**, *12*, 541–545.
[38] H. Endo, H. Cölfen, D. Schwahn, *J. Appl. Crystallogr.* **2003**, *36*, 568–572.
[39] L. M. Qi, H. Cölfen, M. Antonietti, *Angew. Chem.* **2000**, *112*, 617–621; *Angew. Chem. Int. Ed.* **2000**, *39*, 604–607.
[40] L. M. Qi, H. Cölfen, M. Antonietti, *Chem. Mater.* **2000**, *12*, 2392–2403.
[41] L. M. Qi, H. Cölfen, M. Antonietti, M. Li, J. D. Hopwood, A. J. Ashley, S. Mann, *Chem. Eur. J.* **2001**, *7*, 3526–3532.
[42] S. H. Yu, M. Antonietti, H. Cölfen, J. Hartmann, *Nano Lett.* **2003**, *3*, 379–382.
[43] H. Cölfen, L. M. Qi, Y. Mastai, L. Börger, *Cryst. Growth Des.* **2002**, *2*, 191–196.
[44] K. L. Robinson, J. V. M. Weaver, S. P. Armes, E. D. Marti, F. C. Meldrum, *J. Mater. Chem.* **2002**, *12*, 890–896.
[45] S. H. Yu, H. Cölfen, M. Antonietti, *Chem. Eur. J.* **2002**, *8*, 2937–2945.
[46] S. H. Yu, H. Cölfen, M. Antonietti, *Adv. Mater.* **2003**, *15*, 133–136.
[47] M. Öner, J. Norwig, W. H. Meyer, G. Wegner, *Chem. Mater.* **1998**, *10*, 460–463.
[48] A. Taubert, D. Palms, O. Weiss, M. T. Piccini, D. N. Batchelder, *Chem. Mater.* **2002**, *14*, 2594–2601.
[49] A. Taubert, D. Palms, G. Glasser, *Langmuir* **2002**, *18*, 4488–4494.
[50] A. Taubert, C. Kubel, D. C. Martin, *J. Phys. Chem. B*, **2003**, *107*, 2660–2666.
[51] D. B. Zhang, L. M. Qi, J. M. Ma, H. M. Cheng, *Chem. Mater.* **2002**, *14*, 2450–2457.
[52] S. H. Yu, M. Antonietti, H. Cölfen, M. Giersig, *Angew. Chem.* **2002**, *114*, 2462–2466; *Angew. Chem. Int. Ed.* **2002**, *41*, 2356–2360.
[53] F. Bouyer, C. Gerardin, F. Fajula, J. L. Putaux, T. Chopin, *Colloids Surf. A,* **2003**, *217*, 179–184.
[54] S. H. Yu, H. Cölfen, Y. Mastai, *J. Nanosci. Nanotech.* **2004**, *4*, 291–298.
[55] L. Addadi, S. Weinstein, E. Gati, I. Weissbuch, M. Lahav, *J. Am. Chem. Soc.* **1982**, *104*, 4610–4617.
[56] D. Zbaida, I. Weissbuch, E. Shavit-Gati, L. Addadi, L. Leiserowitz, M. Lahav, *React. Polym., Ion Exch., Sorbents*, **1987**, *6*, 241–253.
[57] D. Zbaida, M. Lahav, K. Drauz, G. Knaup, M. Kottenhahn, *Tetrahedron* **2000**, *56*, 6645–6649.
[58] Y. Mastai, M. Sedlak, H. Cölfen, M. Antonietti, *Chem. Eur. J.* **2002**, *8*, 2430–2437.
[59] L. J. W. Shimon, F. C. Wireko, J. Wolf, I. Weissbuch, L. Addadi, Z. Berkovitchyellin, M. Lahav, L. Leiserowitz, *Mol. Cryst. Liq. Cryst.* **1986**, *137*, 67–86.
[60] L. J. W. Shimon, M. Vaida, L. Addadi, M. Lahav, L. Leiserowitz, *J. Am. Chem. Soc.* **1990**, *112*, 6215–6220.
[61] I. Weissbuch, I. Kuzmenko, M. Vaida, S. Zait, L. Leiserowitz, M. Lahav, *Chem. Mater.* **1994**, *6*, 1258–1268.
[62] R. L. Penn, J. F. Banfield, *Geochim. Cosmochim. Acta* **1999**, *63*, 1549–1557.

Received: April 30, 2004
Revised: January 5, 2005
Published online: March 30, 2005

